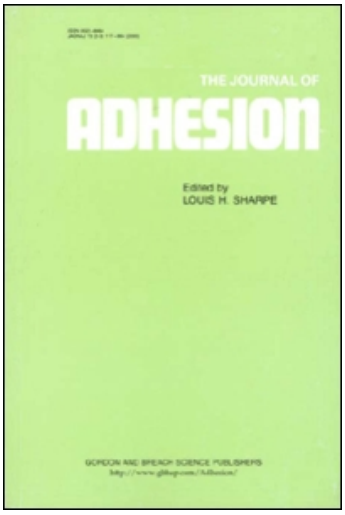

The Journal of Adhesion
Publication details, including instructions for authors and subscription information:
http://www.informaworld.com/smpp/title~content=t713453635

Surface Energy and Adhesion Studies on Acrylic Pressure Sensitive Adhesives

Lihua Li[ab]; Matthew Tirrell[ac]; Gary A. Korba[d]; Alphonsus V. Pocius[d]
[a] Department of Chemical Engineering and Materials Science, University of Minnesota, Minneapolis, Minnesota, USA [b] Applied Materials, Santa Clara, California, USA [c] Departments of Chemical Engineering and of Materials, Materials Research Laboratory, University of California Santa Barbara, Santa Barbara, California, USA [d] Adhesive Technologies Center, 3 M Company, St. Paul, Minnesota, USA

To cite this Article Li, Lihua , Tirrell, Matthew , Korba, Gary A. and Pocius, Alphonsus V.(2001) 'Surface Energy and Adhesion Studies on Acrylic Pressure Sensitive Adhesives', The Journal of Adhesion, 76: 4, 307 — 334
To link to this Article: DOI: 10.1080/00218460108030724
URL: http://dx.doi.org/10.1080/00218460108030724

The Journal of Adhesion, 76:307 - 334, 2001

0021-8464 / 01 $12.00 + .00

Surface Energy and Adhesion Studies on Acrylic Pressure Sensitive Adhesives

LIHUA LI[a, b], MATTHEW TIRRELL[a, c], GARY A. KORBA[d], and ALPHONSUS V. POCIUS [d]

[a]*Department of Chemical Engineering and Materials Science, University of Minnesota, Minneapolis, Minnesota, USA;* [b]*Applied Materials, Santa Clara, California, USA;* [c]*Departments of Chemical Engineering and of Materials, Materials Research Laboratory, University of California Santa Barbara, Santa Barbara, California, USA;* [d]*3 M Company, Adhesive Technologies Center, St. Paul, Minnesota, USA*

(Received 1 September 2000; in final form 16 January 2001)

The surface energy and adhesion dynamics of pressure sensitive adhesives-like networks (PSA-LNs) as mimics for PSAs were studied using JKR-based contact mechanics and peel tests. Acrylic acid (AA) was co-polymerized with 2-ethyl hexyl acrylate (2-EHA) and 1,6-hexane diol diacrylate (HDDA) to create PSA-LNs. The measured surface energy (27 to 31 mJ/m^2) was sensible as surmised from their structure. Acrylic acid content increases the surface energy, threshold adhesion energy and adhesion hysteresis of PSA-LNs. Measurements of adhesion dynamics showed a dependence of adhesion energy to the 0.6 – 0.8 power of crack speed, depending upon the model chosen for analysis of the data. When compared with actual pressure-sensitive adhesive tape peel tests, the adhesion dynamics data predicted the peel strength. This study shows a direct relationship between threshold adhesion energy, crack propagation mechanics and peel strength measurements.

Keywords: Surface energy; Threshold adherence energy; Pressure sensitive adhesives, Peel adhesion

---

We gratefully acknowledge the financial support provided by 3M Company and the NSF-MRSEC DMR-9809364 at the University of Minnesota. We thank Prof. Christopher Macosko, Prof. William Gerberich and Dr. Afshin Falsafi for stimulating discussions.

Presented at the session of the 23rd Annual Meeting of The Adhesion Society, Inc., held in Myrtle Beach, South Carolina, USA, 20 – 23 February 2000, honoring Pierre-Gilles de Gennes, the recipient of The Adhesion Society Award for Excellence in Adhesion Science, sponsored by 3M.

Address correspondence to Alphonsus V. Pocius, 3M Company, Adhesive Technologies Center, St. Paul, MN 55144, USA. E-mail: avpocius1@mmm.com

INTRODUCTION

Acrylic Pressure Sensitive Adhesives (PSAs) are used widely in industry. These PSAs are made from appropriately chosen combinations of acrylic monomers yielding soft and tacky polymers of low glass transition temperature (T_g). Suitable monomers commonly reported in the patent literature are alkyl acrylates and methacrylates of 4–17 carbon atoms, for example, 2-ethyl hexyl acrylate (2-EHA) ($T_g \sim -70°C$). To control the adhesive properties of PSAs, the acrylic esters are almost always co-polymerized with other monomers with generally higher T_g or with proper functionality [1]. Acrylic acid (AA) has often been added as a secondary monomer, its homopolymer having a T_g of 106°C. Use of acrylic acid provides a co-polymer having carboxyl groups to provide cross-linking sites. A typical acrylic PSA composition is 5–90% of a major monomer, 10–40% of a modifying monomer, and 2–20% of a monomer with desired functional groups [2, 3].

Composition plays an important role in the practical adhesive bonding characteristics of acrylic PSAs. Copolymerization of various monomers is the universally used technique to vary adhesive properties. Natural rubber and other rubbery materials can be compounded to form pressure sensitive adhesives by the addition of tackifying resins and plasticizers. The exact mechanism of the composition effect on adhesive properties is poorly understood but it is known that the properties of a pressure sensitive adhesive depend primarily on the viscoelastic nature of the adhesive mass. Many commercial pressure sensitive adhesives are a blend of a base polymer and, at least, a tackifying resin. A good tackifying resin is designed to modify the viscoelastic properties of the adhesive in order to provide tack.

Although proper viscoelasticity is a prerequisite for practical adhesion of PSAs, it is not the only factor that affects adhesion. For adhesion to many substrates, the surface energy of the adhesive layer becomes important. To be effective, a pressure-sensitive adhesive must be able to immediately wet the surface with which it is brought into contact [4]. Therefore, the relationship between the surface energy of the adherend and the surface energy of the adhesive becomes important. Unfortunately, the surface energy of PSAs is not directly measurable. Although the surface energy of high polymers has been

estimated by contact angle experiments, this cannot be done for typical PSAs. Data generated by contact angle for pressure sensitive adhesives are unreliable due to the solubilization of low polarity testing liquids into the PSA [2]. Use of high polarity, hydrogen-bonding liquids may lead to significant error due to the insufficient theoretical interpretation of contact angle measurements. In addition, even for insoluble liquids, the liquid-like character of PSAs at long times of contact will cause the formation of a lens. This confounds simple analysis of contact angle data [5].

Surface energy of a pressure sensitive adhesive can be measured indirectly, however. Zosel [6] showed that pressure sensitive adhesion to a substrate obeyed the following conditions: if $\gamma_{adhesive} \geq \gamma_{substrate}$, then measured adhesion would be dependent on the surface energy of the substrate. If $\gamma_{adhesive} < \gamma_{substrate}$, then adhesion would be independent of substrate surface energy. The value at which adhesion becomes independent of substrate surface energy becomes an estimate of the adhesive surface energy, $\gamma_{adhesive} \approx \gamma_{substrate}$. Direct measurement of the surface energy of PSAs has been a challenge.

Destructive mechanical tests are usually employed to determine practical adhesion strength. Adhesion tests resemble fracture experiments in that the description of the strength of bonding can be formulated from the energy balance criterion of Griffith. However, the nature of crack propagation in many adhesives is different from simple cohesive failure of brittle solids. The fracture energies are found to depend upon speed of deformation and test temperature in the same way that dissipative properties do. This feature is particularly pronounced for viscoelastic adhesives [7]. To study intrinsic adhesion, one must minimize rate dependent effects. Gent and Schultz [8] proposed that the measured strength of adhesion is composed of two terms: the thermodynamic work of adhesion, W_a, and a dissipation function, f(v), as shown in Eq. (1), where v is the rate of crack propagation and f(v) is a function of v reflecting energy expended in irreversible processes. This idea was extended by Andrews [9]. He proposed a generalized fracture theory, as shown in Eq. (2), where Φ is a loss function that depends on the crack growth rate, v, temperature, T, and strain level, *e*. G_0 is the threshold adhesion energy, which is commonly larger than W_a. G is the energy required to propagate a crack through an adhesive contact. We call G the "adhesion energy".

At zero rate conditions and in situations where the contact is reversible, G_0 and W_a should be the same.

$$G_a = W_a f(v) \tag{1}$$

$$G = G_0 \Phi(v, T, e) \tag{2}$$

Thus, in Eq. (2) surface properties (G_0) and viscoelastic properties are decoupled from elastic properties, geometry, and loading conditions that are included in G. The dimensionless "dissipation function", Φ, is a characteristic of crack propagation in the material. In theory, once Φ is known, Eq. (2) may allow one to predict features such as kinetics of detachment at fixed load, fixed grips, or fixed crosshead velocity.

The dissipative component, which becomes significant at crack speeds even as low as 1 μm/s [10], embodies molecular dissipation of mechanical energy at the interface or interfacial viscoelastic deformations (typically $10^2 - 10^3$ J/m^2) [11], as well as chain scission (about 1 J/m^2) [12]. Equation (2) implies that in order to obtain G_0 from a standard mechanical test of practical adhesion, one would need to perform such measurements under "threshold conditions", *i.e.*, at sufficiently low rates of detachment that the measured adhesion is rate independent. It is not clear at present whether such a threshold is attainable with $v > 0$ [13].

Direct measurement of surface energies *via* contact mechanics methods based on the JKR theory has proven to be successful and accurate for surfaces and interfaces of elastic materials [14]. According to the JKR theory, the contact radius, a, between contacting spherically symmetric bodies under an applied load, P, is given by

$$a^3 = \frac{R}{K}\left[P + 3\pi WR + \sqrt{6WRP + (3\pi WR)^2}\right] \tag{3}$$

In which:

$$\frac{1}{K} = \frac{3}{4}\left(\frac{1-\nu_1^2}{E_1} + \frac{1-\nu_2^2}{E_2}\right) \tag{4}$$

$$\frac{1}{R} = \frac{1}{R_1} + \frac{1}{R_2} \tag{5}$$

where a is the radius of contact, P is the applied load, R is a radius of curvature, E and ν are the tensile moduli and the Poisson's ratios of the materials in test. In the case of self-adhesion, W, the intrinsic work of adhesion, is twice the surface energy, γ, as shown in Eq. (6). In the case of adhesion between dissimilar materials, the work of adhesion is described by Eq. (7), where γ_1, γ_2 and γ_{12} are, respectively, the surface energy of material 1 and 2, and the interfacial energy between 1 and 2.

$$W_{11} = 2\gamma_{11} \tag{6}$$

$$W_{12} = \gamma_1 + \gamma_2 - \gamma_{12} \tag{7}$$

Our PSA-like network (PSA-LNs) samples are in the form of cylinders. This choice was made on the basis of the chemistry and composition control required of our samples, as is explained in the synthesis and sample preparation section. The case of contact between two crossed cylinders of equal radii, R_c, as illustrated in Figure 1 is identical to a sphere of $R_s = R_c$ in contact with a flat surface of $R_f = \infty$, *i.e.* [15],

$$\frac{1}{R} = \frac{1}{R_s} + \frac{1}{R_f} = \frac{1}{R_c} \tag{8}$$

Inverting Eq. (3) yields Eq. (9), where G is the energy release rate, or effective adhesion energy. Thus, G can be obtained by monitoring the contact radius as a function of the applied load, provided R and K are

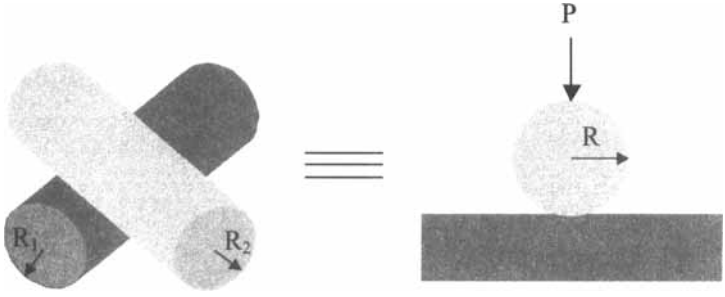

FIGURE 1 Crossed-cylinder contact geometry used in this study is equivalent to contact between a sphere and a flat. See text for definitions of symbols.

known. We note that the original JKR derivation uses W in place of G in Eqs. (3) and (8); however, this original expression holds true only when the thermodynamic equilibrium conditions established by the initial contact of the two surfaces are sustained over the duration of the experiment. Maugis and Barquins [16] extended JKR theory to include non-equilibrium behavior common in unloading processes by invoking linear fracture mechanics arguments. The form of the equations is valid only when the crack propagates at the interface and gross displacements are purely elastic.

$$G = \frac{((a^3K/R) - P)^2}{6\pi a^3 K} \tag{9}$$

A desirable feature of contact mechanical experiments is the very low crack propagation speeds that are accessible. Another feature is their capability to reveal both thermodynamic and kinetic information through loading and unloading cycles. Acrylics, as model polymers, allow the exploration of the relative effects of surface and rheological behavior as a function of composition and temperature. At such low speeds and elevated temperatures, it is possible to access the threshold adhesion energy, which enables us to understand further the dissipation function, Φ.

This study addresses the effect of acrylic acid on surface energy, adhesive behavior and mechanical properties of PSAs. The challenge in this research is the inherent viscoelastic nature of a PSA. To get around this problem, PSAs were cross-linked to create Pressure Sensitive Adhesive-like Networks (PSA-LNs). Another purpose of this research is to develop an elastic foundation, other than cross-linked poly (dimethyl siloxane) (PDMS), to be used in JKR measurements in order to get away from possible PDMS contamination. The surface energies of PSA-LN without acrylic acid and with 10 wt% acrylic acid were measured using the JKR method. The interplay of the effect of acrylic acid, temperature and rate on the adhesive behavior of PSA-LNs was studied systematically. Rheological properties of the PSA-LN provide insight into the adhesion measurement results. Surface composition and cleanliness was investigated using small-spot X-ray Photoelectron Spectroscopy (XPS) analysis. Finally, standard peel tests were used to investigate the correlation between the threshold adhesion energy and practical adhesive bond strength.

MATERIALS AND EXPERIMENTAL TECHNIQUES

Preparation of Pressure Sensitive Adhesive-like Networks

Pressure sensitive adhesive-like networks (PSA-LNs) were synthesized for use in the JKR adhesion tests. Acrylic acid (AA) was co-polymerized with 2-ethyl hexyl acrylate (2-EHA) as described in Table I. In order to provide elasticity necessary for simple contact mechanics, 10% 1,6-hexane diol diacrylate (HDDA) di-functional monomer was used to cross-link the material. The choice of HDDA as cross-linker was based upon reactivity ratios of monomers. Use of HDDA as a cross-linker provides the best chance to have a random copolymer with minimal blockiness.

Free radical polymerization was employed to synthesize acrylic PSA-LNs. Inhibitors were removed using molecular-sieve packed columns. Monomers were then purged with high-purity argon and transferred to an argon-purged glove box to avoid any oxygen sorption that would poison the free radical polymerization. The concentration of free radical initiator, azo-bis-isobutyronitrile (AIBN) was 0.2 wt%. To avoid compositional changes due to selective volatility of monomers in the course of the reaction, the samples were confined in sealed tubes during polymerization [17]. The tubes were 1-mm radius quartz capillary tubes. The fragile, filled tubes were capped with extreme care so as not to exert extra force. The samples were then taken out of the glove box and placed in a convection oven. The polymerization reaction was carried out at 80°C for 24 hours.

Breaking the capillary tubes and immersing them in ethyl acetate released the PSA-LN cylinders. Polymerization shrinkage due to decrease in molar volume in acrylate systems is substantial and this provided a means for easy removal of the cross-linked cylinder from

TABLE I The composition of PSA-like network cylinders

Sample designation	*Monomer (wt%)*	*Co-monomer (wt%)*	*Cross-linker (wt%)*
	2-EHA	AA	HDDA
PSA-LN-NoAA	90	0	10
PSA-LN-10AA	80	10	10

the quartz tube. Ethyl acetate is a good solvent for acrylic PSAs and makes them swell, thus freeing themselves from the shattered quartz tubes. The swollen cylinders of PSAs were soaked in fresh ethyl acetate for a few days and then subjected to Soxhlet extraction in order to remove low molecular weight or unreacted species. The cylinders were stored in the soaked state and were cut in pieces of approximately 10 mm length. Cylinders were transferred onto a glass slide in a clean glass Petri dish that was partially filled with ethyl acetate. This provides a saturated environment for slow drying of samples that would otherwise break or crack with rapid drying.

Preparation of Pressure Sensitive Adhesive Tapes

For the investigation of the correlation between the intrinsic work of adhesion and practical adhesion strength, PSAs with similar co-monomer content were synthesized. These PSAs were coated onto a backing to generate a pressure-sensitive adhesive tape (PSAT) similar to commercial materials. In order for the adhesive chemistry to operate as a PSAT, the cross-link density was much lower than that of the PSA-LNs.

PSATs were generated using monomer formulations as close as possible to the PSA-LNs but having cross-link density similar to that used in commercial acrylic PSATs. To accomplish this, 2-ethyl hexyl acrylate or a combination of 90% 2-ethyl hexyl acrylate and 10% acrylic acid were dissolved at 50 wt% in ethyl acetate. Each container was flushed with nitrogen for 10 minutes in order to reduce dissolved oxygen in the reaction mixture. The containers were sealed and placed in an Atlas "Launder-ometer" (Atlas Electric Device Co, Chicago IL) to remain at a constant temperature at 80°C for 48 hours.

1% benzoyl peroxide (by weight of polymer) was dissolved into each polyacrylate/ethyl acetate solution. Each ethyl acetate solution was coated onto a piece of poly(ethylene terephthalate) film (0.051 mm thick). The coated adhesive was allowed to air dry for 30 minutes before being placed in an oven pre-set at 150°C. The adhesive was allowed to dry and cross-link further under these conditions for 45 minutes. This provides a PSAT having chemistry similar to the PSA-LNs, but with much lower crosslink density. The adhesive thickness on the poly(ethylene terephthalate) film was 0.032 mm. The

PSATs made in this fashion were stored in a constant temperature (75°F) and constant humidity room (85% RH) for at least 24 hours before assembling the test specimens.

The JKR Apparatus and Environmental Cell Design

A homemade, automated JKR apparatus, as shown in Figure 2, is used in this study to perform adhesion tests. A micrometer is connected to a precision translation stage to control the displacement. An analytical balance measures the corresponding load. The CCD camera captures the contact area. Adhesion tests were performed at controlled humidity, close to zero. The temperature cell enables us to run adhesion tests at temperatures as high as 250°C. The whole assembly is mounted on an anti-vibration table. A more detailed diagram of the apparatus is given in Ref. [18].

Adhesion Measurement Procedure: a Contact Mechanical Approach

The two cylindrical samples were glued to supporting surfaces by applying small amounts of thoroughly-mixed, fast-setting epoxy. After reaching thermal equilibrium and complete curing of the epoxy,

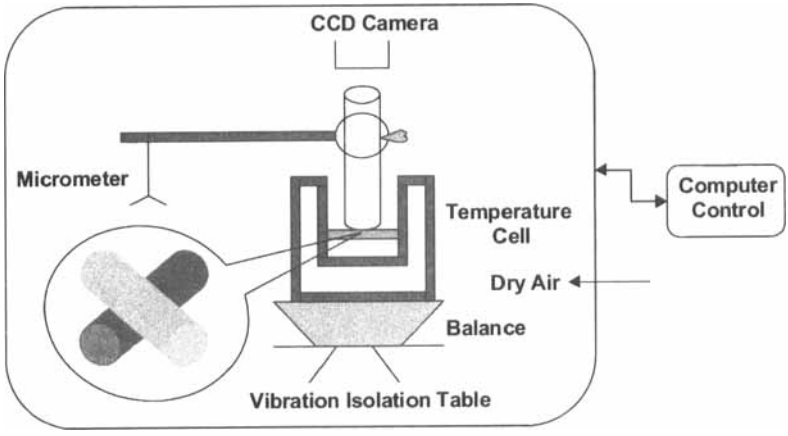

FIGURE 2 A schematic of the environmental cell in the JKR apparatus.

sample cylinders were crossed by close examination at low magnification. A slight contact was made in order to align the video-zoom with the center of contact. Cylinders were then separated and the system was allowed to equilibrate mechanically and thermally for at least 3 hours. Samples were compressed stepwise, allowing time for equilibration between each step. After a 10-step compression of 1 μm at each step and equilibration at the maximum load for 30 minutes, samples were decompressed in a similar stepwise fashion. For crack propagation rate studies, steady unloading at vertical separation speeds ranging from 1 nm/s to 100 nm/s was used. Measurements were run at both room temperature and an elevated temperature of 75°C. The displacement, load and contact area were recorded on the computer for data analysis. The radius of the cylinders was measured sideways under a light microscope.

Practical Adhesion Tests

Glass plates of nominal 1/4″ (0.64 cm) thickness were cleaned by scrubbing under solvent and then Alconox™/water. The surfaces were rinsed with de-ionized water and finally reagent-grade acetone. Glass plates (cleaned as described above) were further subjected to 10 minutes of oxygen plasma using a hospital instrument sterilizer (Harrick PDC-32G.) The above-described PSA coating solutions were further diluted to about 9% solids by weight. The 9% solids coating solutions were coated onto the glass slides using a #6 Meyer rod yielding a dry coating thickness of about 1.2 microns. The coated glass plates were placed in an oven at 150°C for 45 minutes.

In the constant temperature/constant humidity room described above, pieces of PSAT (1.27 cm wide) were cut from the larger coated pieces (as described above.). The tape was tacked to one end of the coated glass plate and a 5 lb. (2.3 kg) rubber roller was passed over the tape three times. The sample was immediately affixed to an Instron 4501 tensile testing machine that had been equipped with a 90° peel fixture. This tensile testing machine is computer controlled and was capable of measuring force at a range of pre-determined cross-head speeds. The crosshead speeds used in these measurements were (in

inches/minute): 0.001, 0.005, 0.01, 0.05, 0.1, 0.5, 1, 5, 10 (0.0025, 0.013, 0.025, 0.13, 0.25, 1.3, 2.5, 13, 25 (cm/minute)). The average peel force was measured at each of these peel rates. The instrument was zeroed and calibrated before each run.

Surface Composition Characterization

Surface composition of the PSA-LNs was measured using a Surface Science Labs XPS instrument with small spot capability. Because the samples are hemi-cylinders, there was no specific take-off angle and the measured values must be considered an average surface composition over the first 50 Angstrom or so in depth. The instrument was used to "image" the cylinder (to insure that the substrate was not part of the analysis) and the chemistry was determined near the "crown" of the sample.

The surface chemistry of the PSATs was measured using a Physical Electronics Model 5400 ESCA at a 20 degree take-off angle. The area analyzed is approximately 1 cm × 1 cm. The analysis depth is on the order of 20 Angstrom units.

Rheological Measurements

The rheology of the cylinders, the same as used for adhesion measurements, was studied in parallel-plate geometry in a Rheometrics Solid Analyzer RSA-II™. This analyzer measures the Young's modulus in a uniaxial tension mode. Cylinders, approximately 5 mm in length and 2 mm in diameter, are epoxy-bonded between two opposing rods with a diameter of 7 mm. After pre-tensioning the system by 5 g and establishing thermal and mechanical equilibrium at laboratory conditions, a dynamic strain sweep was performed to test the linear behavior of the PSA-LNs. The frequency was 1 rad/s and the strain range was 0.5–5%. A frequency sweep with a 2% strain was performed in the range of 100–0.01 rad/s. The stress relaxation experiment was also carried out at 2% strain for 1 hour. The temperature ramp was carried out at temperatures between −80°C and 80°C. The frequency sweep tests and stress relaxation experiments were also run at different temperatures.

RESULTS AND DISCUSSION

Surface Composition Analysis

The data taken in XPS analysis of the surfaces used in this work are shown in Figure 3. The small spot size XPS analysis showed us that our contact mechanics specimens were not contaminated with any foreign material. In addition, the analysis demonstrated that the surface composition of these samples is similar to that calculated for the bulk composition of the material. There is an apparent slight excess of hydrocarbon on the surface as was found in previous work [18].

The PSAT surface compositions were also similar to the calculated bulk composition. However, because these measurements were made on a planar surface at a shallow take-off angle, there is an apparently larger hydrocarbon excess in comparison with that calculated for the bulk. It is expected that if angle-resolved measurements could be done for the hemi-cylinders, we would see a similar surface excess of hydrocarbon. Despite the difference in measurement instrumentation, the surface chemical compositions of the PSATs and the PSA-LNs are quite similar.

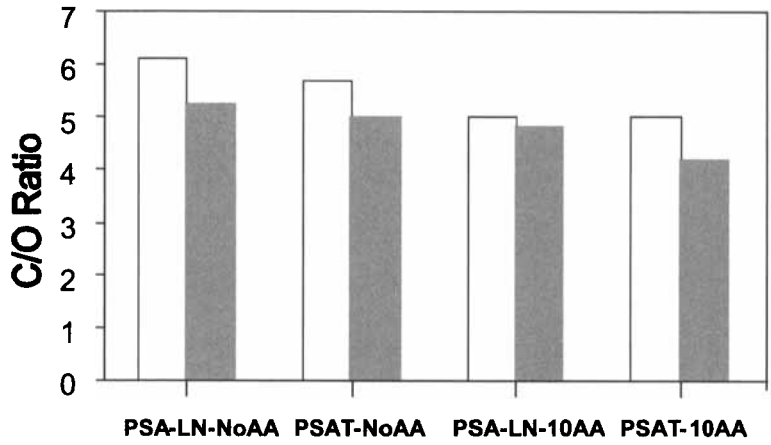

FIGURE 3 Surface chemical composition of PSA-LNs and PSATs. □ indicates measured carbon/oxygen ratio. indicates calculated carbon/oxygen ratio based upon bulk composition.

Surface Energy Measurement on PSA-LN-NoAA

Different kinetic processes for unloading *versus* loading are suggested from JKR plots of self-adhesion of PSA-LN-NoAA, as shown in Figure 4. Each unloading step took 20 minutes to reach a steady value as compared with 5 minutes corresponding to each loading step. There is a finite but small adhesion hysteresis between the loading and unloading cycles. The quasi-static step loading captures the loss-free equilibrium adhesion. The JKR fit of the loading curve gives a work of adhesion of $55.1 \pm 1.5\,mJ/m^2$, which leads to a surface energy of $27.5 \pm 0.8\,mJ/m^2$. This is in reasonable agreement with expectation from the hydrocarbon nature of the surface, as suggested in the XPS study.

The calculated adhesion energies using Eq. (9) from loading and unloading are plotted in Figure 5. Stepwise unloading within 10 minutes after each unloading step reveals a non-equilibrium condition. Constant intrinsic work of adhesion, W, and adhesion energy, G, are obtained for both loading and unloading after full equilibration. 27% adhesion hysteresis exists between the equilibrium values from

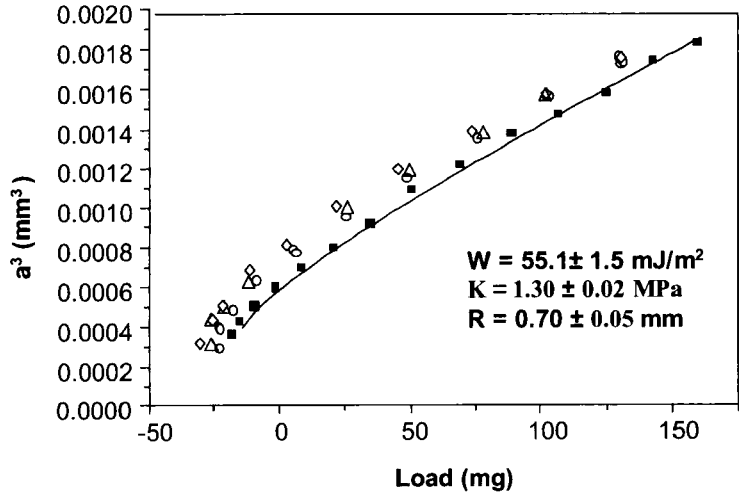

FIGURE 4 JKR plots of self-adhesion of PSA-LN-NoAA at room temperature and zero humidity. The step-loading (■) data points were collected at 1, 5, 10 minutes after each loading step. Unloading data were collected at 1 (○), 10 (△) and 20 (◊) minutes after each unloading step.

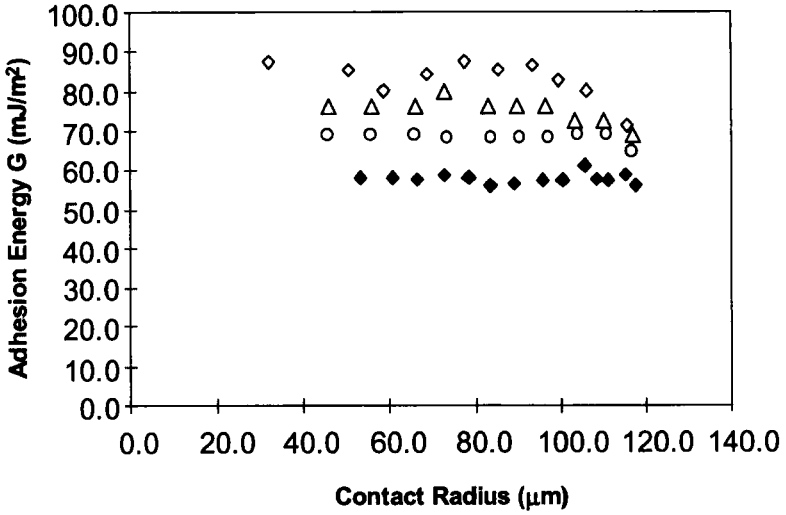

FIGURE 5 The effective adhesion energy calculated from each data point of loading and unloading plotted *versus* corresponding contact radius under room temperature and zero humidity for PSA-LN-NoAA. The step-loading (◆) data points were collected at 1, 5, 10 minutes after each loading step. Unloading data were collected at 1 (○), 10 (△) and 20 (◊) minutes after each unloading step. The uncertainty of the data points is around 15%.

loading and unloading. This might be due to surface rearrangement during contact.

Acrylic Acid Effect on Adhesion of PSA-LNs

As shown in Figure 6, PSA-LN- 1OAA shows a much bigger adhesion hysteresis as compared with that of PSA-LN-NoAA at room temperature. This might be partly due to hydrogen bond formation and surface rearrangement during contact when acrylic acid is present. Another observation is that the adhesion energy from loading is lower than that of PSA-LN-NoAA. A lower surface energy with the addition of acrylic acid seems unlikely. In fact, a value of $30\,mJ/m^2$ does not seem reasonable for the work of adhesion in any case. This measurement would say that the surface energy of the PSA-LN-10AA was $15\,mJ/m^2$, which is less than that of per-fluorinated materials and, hence, unreasonable. It is possible that the greater inelastic nature of the PSA-LN-10AA sample at room temperature

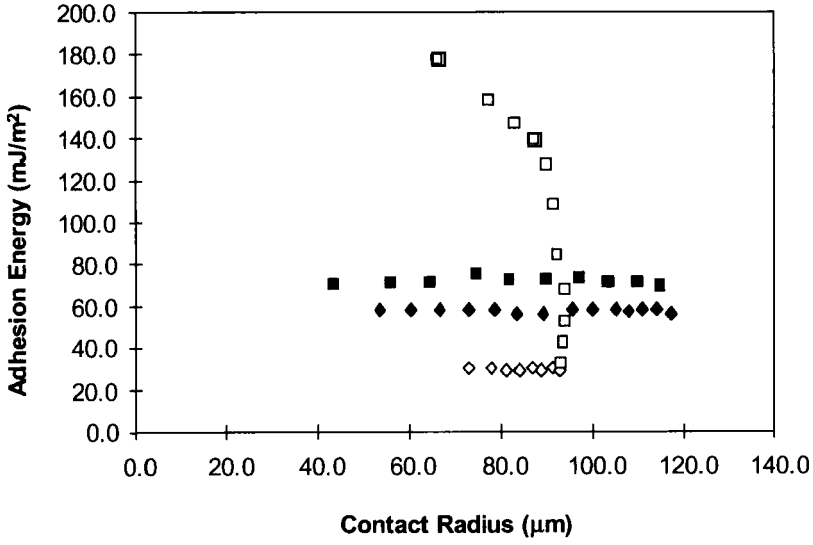

FIGURE 6 A comparison between surface adhesion energy from loading and unloading processes for PSA-LN-NoAA and PSA-LN-10AA at room temperature and zero humidity. NoAA loading (◆), NoAA unloading (■), 10AA loading (◊), 10AA unloading (□). Loading data points were collected at 10 minutes after each step and unloading data were collected 20 minutes after each step. Note the extraordinary adhesion hysteresis for PSA-LN-10AA. The uncertainty of the data points is around 10%.

confounded the use of the JKR method in this analysis. Roberts *et al.* [19] argued that the attainment of true equilibrium is, perhaps, retarded by surface viscoelastic effects. Shanahan [20] suggested that the apparent energy of formation could be lower than the equilibrium value for viscoelastic materials. The work of adhesion obtained from loading corresponds to the apparent energy of formation at finite rate and temperature. On the other hand, viscoelasticity leads to higher apparent energy of debonding from unloading than the equilibrium value. To examine this hypothesis, experiments at different unloading rates and elevated temperatures seemed necessary. For example, acrylic acid was found to increase the effective work of adhesion by a factor of 18 for an acrylic ABA triblock copolymer [21].

To understand the several-fold increase in adhesion energy for the case of PSA-LN-10AA, the dependence of the adhesion energy on crack propagation speed is compared in Figure 7. For the case of

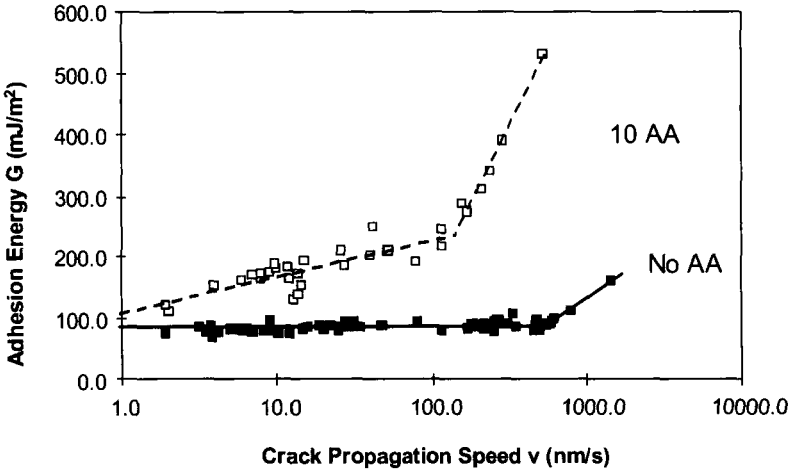

FIGURE 7 The rate dependence of adhesion energy from unloading is plotted *versus* the crack propagation speed for PSA-LN-NoAA (■) and PSA-LN-10AA (□) at room temperature and zero humidity. The unloading vertical separation speeds range from 1, 5, 10, 50 and 100 nm/s, resulting in lateral crack propagation speeds from 1 up to 1000 nm/s. The uncertainty of the data points is around 15%.

NoAA, the adhesion energy does not change with crack speed within the range of 1 to 600 nm/s. The adhesion energy increases with crack speed for crack speeds beyond 600 nm/s. There is a bigger rate dependence of the adhesion energy for the case of PSA-LN-10AA than for PSA-LN-NoAA. An interesting observation is that there is a critical crack propagation speed at which the rate dependence has a transition. This critical rate differs for the two cases. The rate dependence of the adhesion energy at higher crack propagation speed is an indication of a micro-dissipation process at the crack tip – cohesive zone growth. Greenwood and Johnson [22] have predicted that by increasing the velocity of separation, viscoelastic effects extend the length over which the surface forces act, thereby increasing the total force of adhesion

Higher effective adhesion energy is obtained for PSA-LN-10AA than for PSA-LN-NoAA at all finite crack propagation speeds. We suspect that it is related to the formation of hydrogen bonding during contact in the case of PSA-LN-10AA. The curves for 10AA and NoAA can be extrapolated to similar values at lower rates, which are close to the threshold value. This suggests that the effect of AA

addition is primarily that of modification of viscoelasticity and not substantially on the surface energy of these samples. Viscoelasticity is temperature dependent and, hence, it was deemed prudent to make these measurements at an elevated temperature.

Temperature Effect on Self-adhesion of PSA-LN-10AA

As shown in Figure 8 and Figure 9, there is a strong temperature dependence of adhesion and adhesion hysteresis at a higher vertical separation speed of 50 nm/s. The adhesion energy from loading is higher at 75°C than that at 25°C; however, the adhesion hysteresis is lower. Since hydrogen bonds between acrylic acid units break at temperatures above 60°C, acrylic acid becomes labile at 75°C. Thus, the observed temperature effect on adhesion and adhesion hysteresis agrees well with our hypothesis on hydrogen bonding formation during contact.

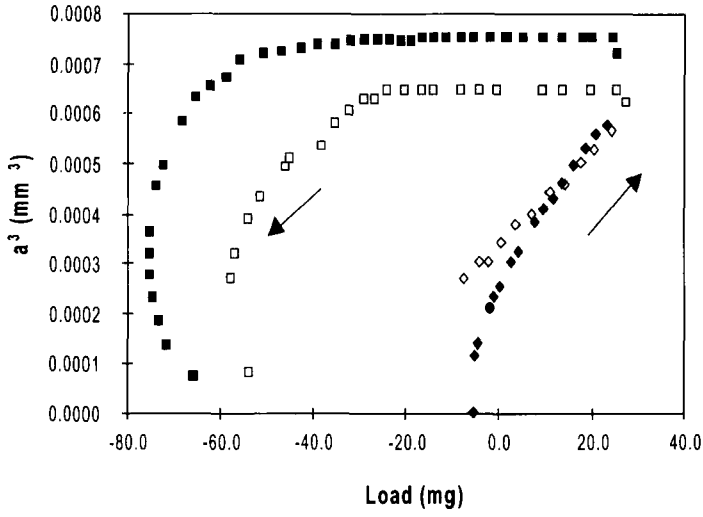

FIGURE 8 JKR plots of self-adhesion of PSA-LN-10AA at room temperature and zero humidity. The step-loading points were collected at 1, 5, 10 minutes after each loading step. Unloading data were obtained at a unloading rate of 50 nm/s. 25°C loading (◆), 25°C unloading (■), 75°C loading (◊), 75°C unloading (□). The uncertainty of the data points is around 10%.

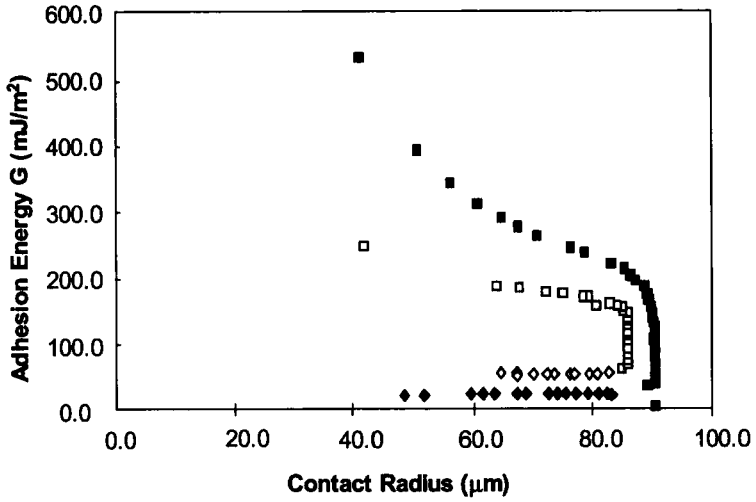

FIGURE 9 Adhesion energy obtained from loading and unloading processes for PSA-LN-10AA at two different temperatures 25°C and 75°C at a vertical separation rate of 50 nm/s. 25°C loading (◆), 25°C unloading (■), 75°C loading (◊), 75°C unloading (□). The uncertainty of the data points is around 10%.

The surface energy of PSA-LN-10AA is $31.5 \pm 1.0\,mJ/m^2$ at 75°C, while the surface energy of PSA-LN-NoAA is $25.1 \pm 0.9\,mJ/m^2$ at 75°C. Thus, acrylic acid additive increases the surface energy of PSA-LNs by 26%. The cohesive strength of the adhesive is also enhanced, which can be observed in dead-load shear tests.

Wu [23] predicted that surface energy decreases linearly with temperature below 200°C. From our data on surface energy of PSA-LN-NoAA, the temperature coefficient ($d\gamma/dT$) is $0.05\,mJ/m^2/°K$. The value of $d\gamma/dT$ does not change much for polymers. Thus, the surface energy of PSA-LN-10AA at 25°C can be estimated as $34\,mJ/m^2$ based on its value at 75°C, but with a larger degree of uncertainty.

As shown in Figure 10, the rate dependence of adhesion energy from unloading for PSA-LN-10AA is smaller at 75°C than at 25°C. There is no obvious transition of rate dependence up to crack opening speeds of 1000 nm/s at 75°C. This can be understood using the WLF shift factor. By raising the temperature, much lower effective testing rates become accessible.

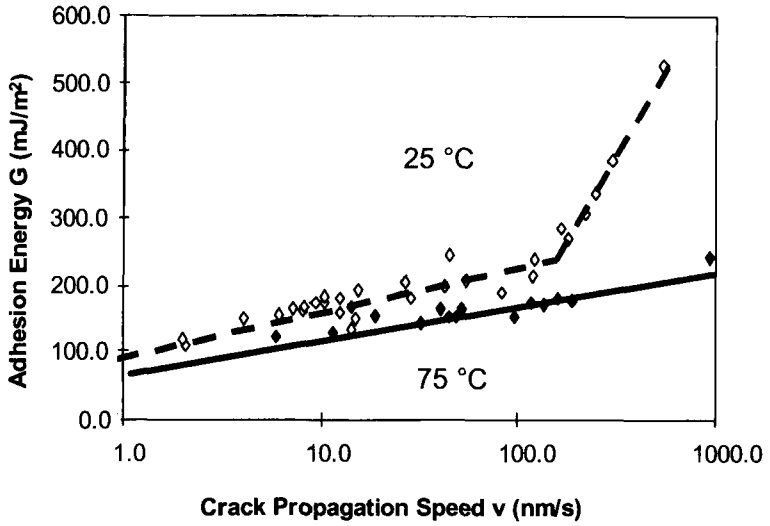

FIGURE 10 The rate dependence of adhesion energy from unloading G is plotted *versus* the crack propagation speed for PSA-LN-1OAA at 25°C (◊) and 75°C (◆) under zero humidity. The vertical separation speeds range from 1, 5, 10, 50 and 100 nm/s, which give lateral crack propagation speeds from 1 up to 1000 nm/s. The uncertainty of the data points is around 15%.

Acrylic Acid Effect on Threshold Adherence Energy and Excess Adhesion Energy

Using the WLF shift factor, we can shift data taken at elevated temperatures to room temperature and, thus, obtain a master curve. As shown in Eq. (10), a_T is the William-Landel-Ferry shift factor for frequency-temperature equivalence,

$$\log a_t = -\frac{8.86(T - T_s)}{101.6 + T - T_s} \tag{10}$$

where $T_s = T_g + 50$, and was first used in fracture mechanics for tearing by Mullins [24]. Master curves generated using shift factors help us to understand the rate dependence at different temperatures. As shown in Figure 11, at very low speed the threshold adhesion energy can be reached. Although acrylic acid addition only increases the surface energy of PSA-LNs by 26%, it enhances the threshold adhesion energy by 100%.

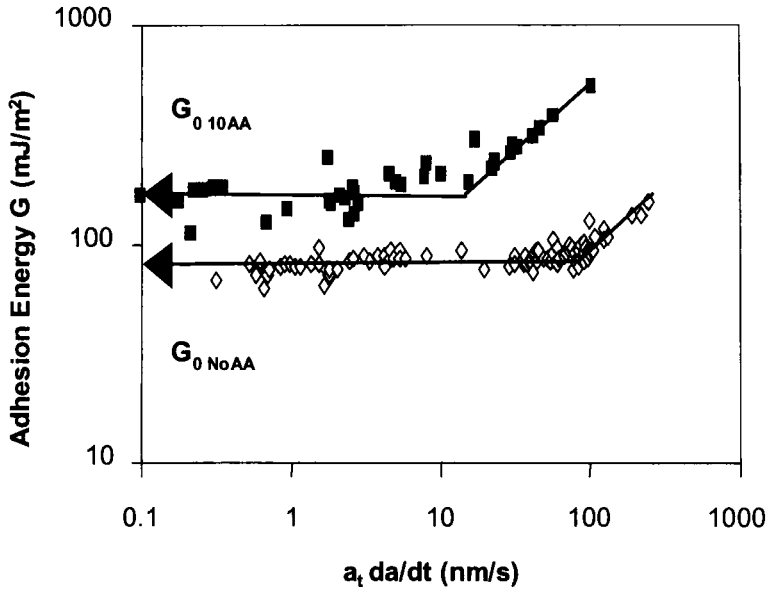

FIGURE 11 The adhesion energy is plotted *versus* the reduced crack speed. The threshold adhesion energy is achieved at very low crack speed for both PSA-LNs with 10AA (■) and without AA content (◊). The uncertainty of the data points is around 20%.

It is interesting to see that PSA-LN-NoAA and PSA-LN-10AA have different reduced critical crack speeds above which the rate dependence of adhesion energy becomes obvious. The rate dependence seems to be similar for these two cases. Our experimental results capture the transition from no rate dependence for zero-rate threshold adhesion energy to finite rate dependence by performing adhesion tests at much lower crack speeds and elevated temperatures. The threshold adherence energy is shown to be attainable at extremely low unloading rates in contact-mechanics-based measurements.

Temperature Effect on Mechanical Properties of PSA-LNs

Rheological measurements were used to verify and understand what we observed in adhesion measurements. As shown in Figure 12, the temperature ramp of PSA-LN-NoAA suggests that PSA-LN-NoAA is

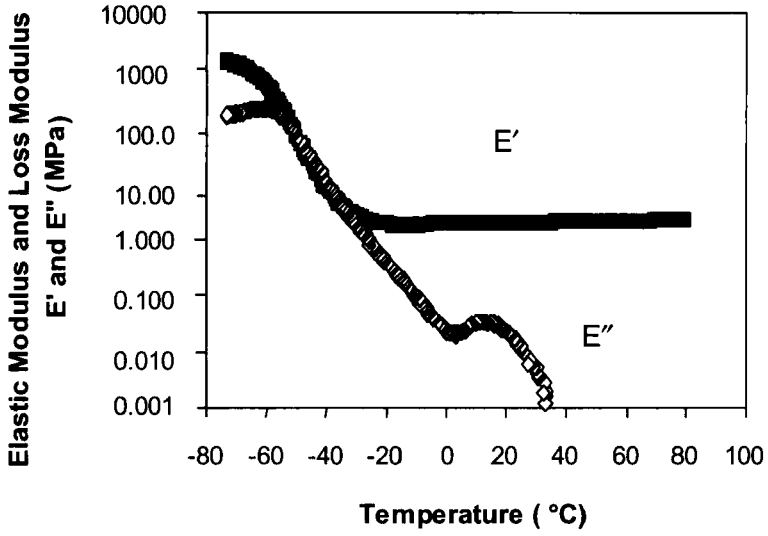

FIGURE 12 Temperature ramp of elastic modulus (■) and loss modulus (◊) for PSA-NoAA. The uncertainty of the data points is around 10%.

an elastic network with very small loss modulus when the temperature is above room temperature. With the addition of acrylic acid, the plateau modulus of PSA-LNs is decreased by about 40%. This result is difficult to interpret but may be due to the fact that the crosslinked structure may inhibit acrylic acid groups from dimerizing. These results are consistent with the elastic constants obtained from the JKR measurements according to the relation of Eq. (4), $E = 9/8\,K$. A value of 0.5 was assumed for Poisson's ratio.

As shown in Figure 13, the elastic modulus of PSA-LN-10AA is lower than that of PSA-LN-NoAA. This figure also shows that, in both cases, the elastic moduli increase with temperature. This can be understood by the dominant entropy effect in an elastic network. According to rubber elasticity theory, the Young's elastic modulus, E, is described by Eq. (11) [25].

$$E = \frac{3\rho RT}{M_C} \tag{11}$$

where ρ is the density, R is the gas constant, T is the absolute temperature and M_C is the molecular weight between crosslinks. Unlike

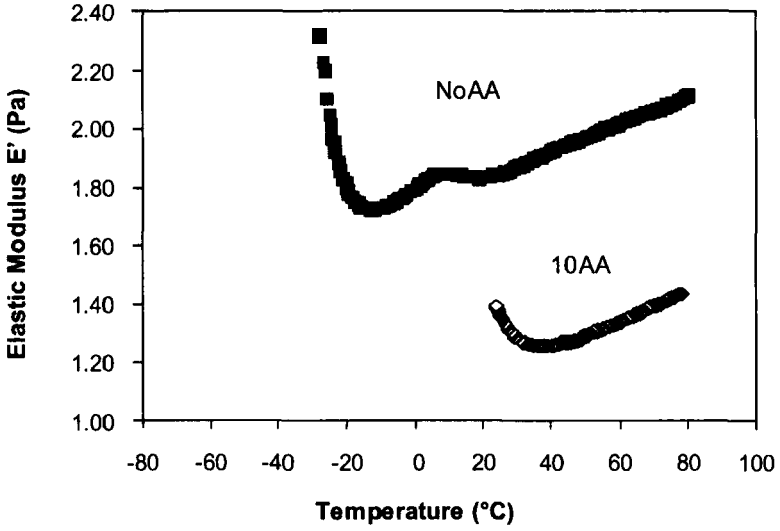

FIGURE 13 Comparison between elastic modulus of PSA-LNs with (◊) and without (■) acrylic acid at a frequency of 1.0 rad/s. The uncertainty of the data points is around 10%.

almost every other material, the modulus of an elastic network increases as the temperature is increased.

As evident in Figure 14, stress relaxation tests show that the Young's modulus is quite flat with time for PSA-LN-NoAA. There is an obvious stress relaxation for PSA-LN-10AA. For this system, the Young's modulus relaxes in ten seconds and then flattens. These results agree with the observation in the JKR measurements that it took much longer for PSA-LN-10AA to reach equilibrium than it did for PSA-LN-NoAA.

As shown in the dynamic frequency sweep (Fig. 15), the elastic modulus of PSA-LN-NoAA does not change with frequency from 0.1 rad/s to 100 rad/s. PSA-LN-10AA does have an increasing elastic modulus at frequencies above 1 rad/s. At very low frequencies, the elastic modulus decreases slightly with the addition of acrylic acid; however, it increases the elastic modulus at higher frequencies. The cross over frequency is around 4 rad/s. The elastic Young's modulus agrees well with the elastic constant measured from adhesion tests according to Eq. (4).

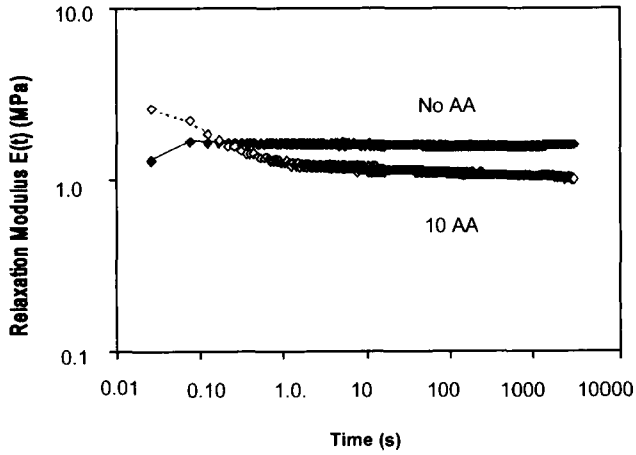

FIGURE 14 Stress relaxation of relaxation modulus for PSA-LN-NoAA (◆) and PSA-LN-10AA (◊). The uncertainty of the data points is around 10%.

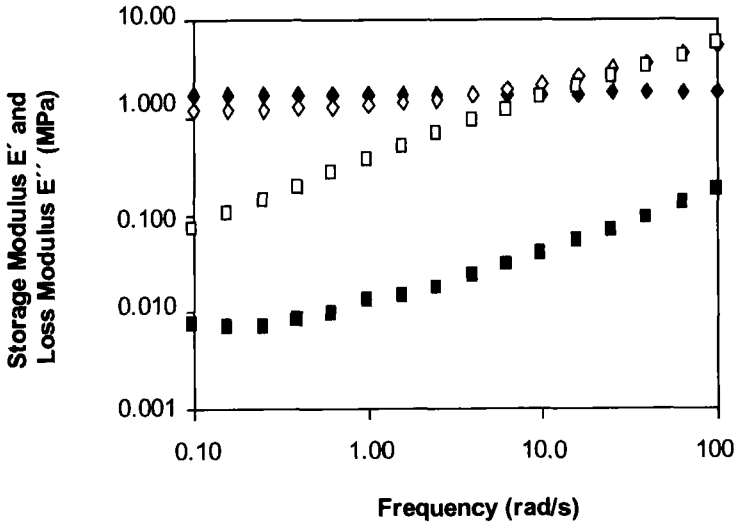

FIGURE 15 From the dynamic frequency sweep, the storage Young's modulus and loss modulus were plotted *versus* frequency for PSA-LN-NoAA and PSA-LN-10AA at 25°C. E′ NoAA (◆), E″ NoAA (■), E′ 10AA (◊), E″ NoAA (□). The uncertainty of the data points is around 10%.

PSA-LN-NoAA shows elastic behavior from both stress relaxation and dynamic frequency sweep tests. The adhesion tests also suggest that PSA-LN-NoAAs behave as elastic materials. Thus, PSA-LN-NoAA can be utilized as an elastic foundation in JKR measurements. Thin films of other materials can be coated on the cylinder, which makes the JKR method applicable to a variety of other materials. In comparison with elastic PDMS networks, this is little or no concern regarding contamination of the sample surface (which can easily happen when using PDMS). We will make use of this practical finding in a future publication.

The Correlation Between the Threshold Adhesion Energy and Peel Adhesion

Figure 16 shows the result of peel measurements using a ninety-degree peel fixture of the PSAT from the PSA itself coated on glass. Apparent

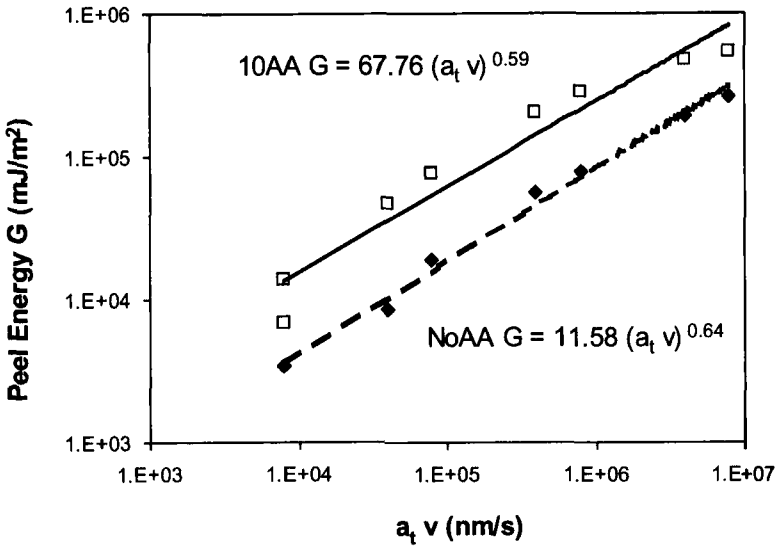

FIGURE 16 Peel energy *versus* reduced peel rates for ninety-degree peel. The cross-head speed ranges from 0.001 to 10 inches/minute. The error bar is not plotted on the log-log plot. The uncertainty of the data points is around 10–20%. The curve fitting suggests a power law dependence of peel energy on reduced peel rate for both PSAT-10AA (□) and PSAT-NoAA (◆).

adhesive failure occurs between the adhesive and the adhesive-coated glass for the cross head speeds tested. The strength of adhesion is characterized by the work of detachment, G, per unit area of growth of the cleavage plane, where G is obtained directly from the peel force, P, per unit width of the test strip [8]. We make the assumption that cross head speed equals crack propagation speed. The peel energy is converted from the peel strength measured at each cross head speed. The peel results clearly show that the co-polymerization of AA with 2-EHA results in an enhancement of the peel strength of the PSAT.

An attempt was made to correlate contact mechanics measurements with the more traditional peel strength measurements. The contact mechanics results are plotted on a graph with the peel measurements in Figure 17. We make a potentially dubious assumption that the micro-mechanics occurring at the peel front is the same as that of a crack propagating in the elastic JKR measurement. Indeed, no account is taken of the stiffness of the backing material in the PSAT. Despite

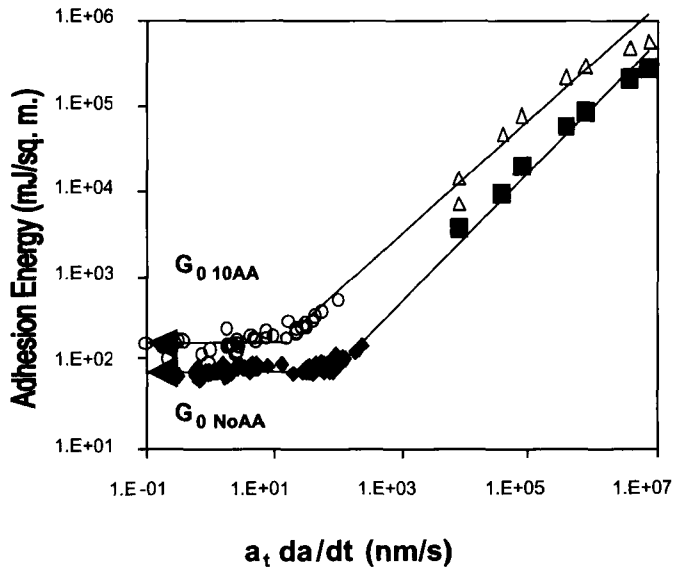

FIGURE 17 The correlation between rate dependence of adhesion energy from peel test and the JKR methods. NoAA-JKR (◆), 10AA-JKR (○), NoAA-peel (■), 10AA-peel (△). The adhesion energy is plotted *versus* the effective crack speeds. Close to parallel curves were obtained for PSA-NoAA and PSA-10AA. The error bar is not plotted on this log-log plot. The uncertainty of the data points is around 10–20%.

these rather substantial omissions, the connection between the JKR results and the traditional peel measurements is striking. The rate dependence is very similar in both the JKR results and peel tests with a power law of $0.5 \sim 0.6$.

In Figure 18, the dissipation function (the reduced excess energy) is plotted as a function of reduced crack speed for PSA-LNs and PSATs, with and without acrylic acid. The dissipation function is obtained using the equation

$$\Phi = 1 + \left(\frac{v}{v^*}\right)^n. \tag{12}$$

where v^* is a characteristic critical crack speed. The data in Figure 18 are the same as the data in Figure 17. However, the curved lines that run through the data are a "best" visual fit of the data using Eq. (12). The parameters used to fit Eq. (12) to the data are shown in Table II. One sees that the presence of acrylic acid in the adhesive increases the threshold adhesion energy by a factor of two and also decreases v^* by

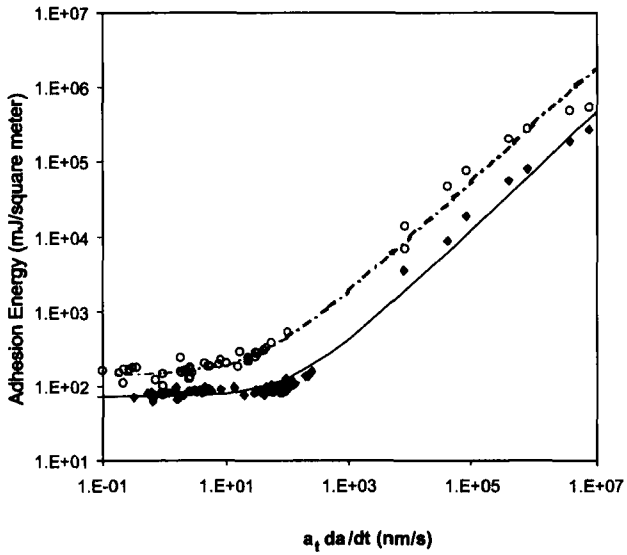

FIGURE 18 The adhesion energy is plotted *versus* the effective crack speeds. NoAA (◆), 10AA (○). The curves are obtained by visually fitting to the formula $G = G_0[1 + (v/v^*)^n]$. For the case of 10AA, $G_0 = 140\,mJ/m^2$, $v^* = 35\,nm/s$, $n = 0.75$. For the case of NoAA, $G_0 = 70\,mJ/m^2$, $v^* = 130\,nm/s$, $n = 0.78$.

TABLE II Fitting parameters used to fit the crack propagation data to Eq. (12)

PSA Type	G_0 (mJ/m^2)	v^* (nm/sec)	n
NoAA	70	130	0.78
10AA	140	35	0.75

a factor of almost four. Maugis and Barquins [16] showed that the dissipation function grew empirically as a power law with the crack velocity to the power 0.6 for the peeling of a polyurethane from a glass surface. This decrease in v^* can be attributed to an increase in the appropriate relaxation times of the elastomer, due to the addition of the acrylic acid groups. This finding is in good agreement with earlier results on poly (n-butyl acrylate) by Ahn and Shull [25] using JKR-type measurements. Using much lower unloading speeds and combined with the peel tests, our results extend the velocity range to values that are both far above and far below v^*.

From the correlation between intrinsic work of adhesion and peel strength, we can conclude that the product of threshold adhesion energy and dissipation function directly determines the peel strength. The intrinsic work of adhesion affects peel adhesion by modifying the threshold adhesion energy. Acrylic acid enhances the peel strength of PSA tapes by increasing the threshold adhesion energy, decreasing the critical crack speed and, thereby, increasing the dissipation function.

CONCLUSIONS

The surface energy and adhesion dynamics of pressure sensitive adhesive-like networks (PSA-LNs) as mimics for PSAs was studied using JKR-based contact mechanics. The measured surface energies were sensible as surmised from their structure. Acrylic acid content dramatically increases adhesion and adhesion hysteresis of PSA-LNs. At elevated temperatures, its effect on adhesion energy and adhesion hysteresis decreases. At the same time, acrylic acid decreases the plateau modulus of these PSA-LNs. The PSA-LN without acrylic acid is shown to be a good elastic foundation that can be used in JKR measurements of release coatings and glassy backing polymers.

Measurements of adhesion dynamics showed a dependence of adhesion energy to the 0.6–0.8 power of crack propagation rate, depending upon the manner in which the data are analyzed. These measurements were compared with peel tests of actual pressure sensitive adhesive tapes. When plotted on the same axes, the peel values were found to be predicted by the adhesion dynamics data. Acrylic acid enhances the peel strength of PSA tapes by increasing the threshold adhesion energy and the dissipation function. This is one of the few examples of the correlation between fundamental adhesion and practical adhesive bond strengths.

References

[1] Ulrich, E. W., *U.S. Patent 2,884, 126* (1959).
[2] Satas, D., *Handbook of Pressure Sensitive Adhesive Technology* (Van Nostrand Reinghold, New York, 1989), 2nd edn., Chap. 15, pp. 396–443.
[3] Creton, C., *Processing of Polymers* (VCH, Weinheim; New York, 1997), Chap. 15, pp. 709–741.
[4] Krenceski, M. A., Johnson, J. F. and Temin, S. C., *JMS-Rev. Macromol. Chem. Phys.* **1**, C26, 143 (1986).
[5] Shanahan, M. E. R., *J. Phys. D: Appl. Phys.* **23**, 703 (1990).
[6] Zosel, A., *Colloid Polym. Sci.* **263**, 541 (1985).
[7] Gent, A. N. and Petrich, R. P., *Proc. Royal Society A* **310**, 433 (1969).
[8] Gent, A. N. and Schultz, J., *J. Adhesion* **3**, 281 (1972).
[9] Andrews, E. H., *J. Mater. Sci.* **9**, 887 (1974).
[10] Kendall, K., *J. Adhesion* **5**, 179 (1973).
[11] Deruelle, M., Leger, L. and Tirrell, M., *Macromolecules* **28**, 7419 (1995).
[12] Ji, H. and de Gennes, P.-G., *Macromolecules* **26**, 520 (1993).
[13] Shanahan, M. E. R. and Michel, F., *Int. J. Adhesion Adhesives* **3**(11), 170 (1991).
[14] Johnson, K. L., Kendall, K. and Roberts, A. D., *Proc. R. Soc. Lond. A* **324**, 301 (1971).
[15] Johnson, K. L., *Contact Mechanics* (Cambridge University Press, Cambridge, 1985), Chap. 4, pp. 84–106.
[16] Maugis, D. and Barquins, M., *J. Phys. D: Appl. Phys.* **11**, 1989 (1978).
[17] Falsafi, A., *Doctoral Thesis* (University of Minnesota, Minneapolis, 1998), Chap. 5, pp. 132–158.
[18] Falsafi, A., Tirrell, M. and Pocius, A. V., *Langmuir* **16**, 1816 (2000).
[19] Roberts, A. D. and Thomas, A. G., *Wear* **33**, 45 (1975).
[20] Shanahan, M. E. R. and Carre, A., *Langmuir* **11**, 1396 (1995).
[21] Flanigan, C. M., Crosby, A. J. and Shull, K. R., *Macromolecules* **32**, 1251 (1999).
[22] Johnson, K. L. and Greenwood, J. A., *J. Coll. Interface Sci.* **192**, 326 (1997).
[23] Wu, S., *Polymer Interface and Adhesion* (Dekker, New York, 1982), Chap. 3, pp. 67–132.
[24] Mullins, L., *Trans. Inst. Rubber Ind.* **35**, 213 (1959).
[25] Young, R. J. and Lovell, P. A., *Introduction to Polymers* (Chapman & Hall, New York, 1991), Chap. 5, pp. 310–424.
[26] Ahn, D. and Shull, K. R., *Langmuir* **14**(13) (1998).